

Antiferromagnetic Order and Phase Coexistence in Antisite Disordered Double Perovskites

Viveka Nand Singh and Pinaki Majumdar

Harish-Chandra Research Institute, Chhatnag Road, Jhusi, Allahabad 211019, India

(Dated: 9 Sep, 2010)

In addition to the well known ferromagnetism, double perovskites are also expected to exhibit antiferromagnetic (AF) order driven by electron delocalisation. This has been seen in model Hamiltonian studies and confirmed via *ab initio* calculations. The AF phases should occur, for example, on sufficient electron doping of materials like $\text{Sr}_2\text{FeMoO}_6$ (SFMO) via La substitution for Sr. Clear experimental indication of such AF order is limited, possibly because of increase in antisite disorder with La doping on SFMO, although intriguing signatures of non ferromagnetic behaviour are seen. We study the survival of electronically driven antiferromagnetism in the presence of spatially correlated antisite disorder and extract the signals in magnetism and transport. We discover that A and G type AF order, that is predicted in the clean limit, is actually suppressed *less strongly* than ferromagnetism by antisite disorder. The AF phases are metallic, and, remarkably, more conducting than the ferromagnet for similar antisite disorder. We also highlight the phase coexistence window that connects the ferromagnetic regime to the A type antiferromagnetic phase.

I. INTRODUCTION

The double perovskites¹⁻³ (DP) are materials of the form $\text{ABO}_3\text{AB}'\text{O}_3$. The B and B' are usually transition metal ions, while A is a rare earth or alkaline earth. The itinerant electrons in this system are coupled strongly to the transition metal magnetic moments, which act as core spins, and the magnetic order is driven^{4,5} by minimisation of the electronic energy, rather than a short range interaction between the moments. Much of the excitement in the double perovskites has been due to the high ferromagnetic T_c , noticeable magnetoresistance, and the possibility of spin polarised conduction in materials like $\text{Sr}_2\text{FeMoO}_6$ (SFMO).

While the ferromagnetism is certainly useful, one may wonder about the occurrence of other kinds of magnetic order in these materials. For example, even 'simple perovskite' transition metal oxides, the cuprates, manganites, or cobaltates, have a rich phase diagram⁶, with a strong dependence on the doping level. The manganites, for instance, exhibit not just ferromagnetism, but also 'CE' magnetic order and A, C, and G type antiferromagnetic (AF) phases⁷, depending on the hole doping level. It is interesting to explore if non-ferromagnetic ordered states are possible in the double perovskites as well.

A study of the model Hamiltonian of these materials shows that at low electron density a ferromagnetic (FM) alignment of the core spins is favoured since it leads to the maximum bandwidth. However, at sufficiently large band filling, antiferromagnetic (AF) states with A or G type order (in two dimensions) successively become favoured⁸⁻¹⁰. While these spin configurations lead to smaller electronic bandwidth they have a higher density of band edge states compared to the ferromagnet.

We have studied these magnetic states in two dimensions⁸ and three dimensions¹¹ elsewhere. *Ab initio* calculations using simple collinear arrangement of the 'core spins' predict similar results^{9,10} in the context of real materials. Nevertheless, electronically driven AF or-

der continues to be elusive experimentally. One can anticipate two reasons: (i) the AF phase occurs at (high) electron densities which have not been probed yet, or (ii) increasing electron density leads to a rapid growth in antisite disorder (ASD), strongly suppressing any signature of long range AF order.

The theoretical effort till now has focused on AF order in the ideal structurally ordered background, where the B and B' ions of $\text{A}_2\text{BB}'\text{O}_6$ alternate along each axis. The situation in the real material is far from ideal, and the B, B' alternation is interrupted by an antiphase boundary (APB)^{12,13} involving BB or B'B' nearest neighbours. This leads to a pattern of structural domains. The ASD not only destroys periodicity but also brings into play an additional AF superexchange coupling when two B ions (like Fe) adjoin each other. If this superexchange scale is sufficiently large, the BB antiphase boundary also acts as a magnetic domain wall¹² (MDW). The effect of such AF superexchange in the double perovskite ferromagnets is well known. There it leads to magnetic domain formation, suppressing the magnetisation, and large enhancement of the resistivity^{14,15}. The interplay of antisite disorder and AF superexchange with *itinerant electron antiferromagnetism* is unexplored.

This paper provides a systematic exploration of the effect of increasing antisite disorder on the AF phases in a two dimensional (2D) double perovskite model. We work in 2D for ease of visualisation and to access large system size.

The phase diagram mapping out the occurrence of AF phases in the 'clean' limit has been established earlier⁸. Here we focus on a couple of electron densities, one each in the 'A type' and 'G type' window, respectively, and study the magnetic order and transport for increasing antisite disorder. Our principal results are the following. (i) The suppression of magnetic order with ASD is *slower* in the AF phases compared to the ferromagnet, and even with $\sim 30\%$ mislocation there are clear signatures of long range order. (ii) The T_c is not significantly

affected, until strong disorder, although the ‘transition’ is broadened. (iii) Both AF phases are metallic, and the increase in their resistivity with ASD is *weaker* than in the ferromagnet. (iv) The phase separation regime between the FM and A type phase is converted to a *phase coexistence* window in the presence of moderate ASD, and one observes the occurrence, locally, of both kinds of order in the same sample.

The paper is organised as follows. We first quickly review the results on AF phases obtained in model studies and *ab initio* calculations, and follow it up with a survey of the few experiments in this regime. We then discuss the model and method. This is followed by a discussion of our results on the AF order in the background of antisite disorder, with focus on the spatial correlations and the transport properties of the system. We conclude with a discussion of the phase coexistence region that intervenes between the ferromagnetic and A type phase, and is likely to be of relevance in La doped SFMO.

II. STUDIES ON AF ORDER

Early studies using model Hamiltonians for double perovskites had observed the instability⁵ of the ferromagnetic state, without exploring the competing phase that emerges. A subsequent variational study¹⁶ did identify non-ferromagnetic phases. More recent studies using both simple models⁸ and realistic DFT calculations^{9,10} indicate that the ferromagnet becomes unstable to an A type phase on increasing electron density. In $\text{Sr}_{2-x}\text{La}_x\text{FeMoO}_6$, for example, this is expected to happen for $x \gtrsim 1$. The DFT studies have employed supercells for a few commensurate doping levels. Using a three band model Hamiltonian, with parameters inferred from the DFT, the authors have explored⁹ a more continuous variation of La doping level and confirmed the DFT trends. The crossover to a non FM ordered state is, therefore, not an artifact of a single band model or two dimensionality that earlier studies employed. As for the effect of ASD on non ferromagnetic phases, we are aware of only one study involving uncorrelated antisite defects¹⁶. It is more focused on the doping dependence, and explores mainly the magnetism, but the trends are consistent with what we observe here.

Samples have indeed been synthesised with large La doping on SFMO^{17,18}. The main observations are (i) a suppression¹⁷ of the low field magnetisation with increasing x , and (ii) a large difference¹⁸ between the field cooled (FC) and zero field cooled (ZFC) response. There is unfortunately no detailed understanding of the ASD in these samples yet (for example via XAFS), or data on resistivity and magnetoresistance.

III. MODEL AND METHOD

The model we study has been presented earlier in the context of the ferromagnetic phase, so we only provide a brief description for completeness.

The information about the B, B’ structural motif is encoded in a binary variable η_i , with $\eta_i = 1$ for B sites and $\eta_i = 0$ for B’ sites. In the structurally ordered DP the η_i alternate along each axis. We will consider progressively ‘disordered’ configurations, generated through an annealing process. For any specified $\{\eta\}$ background the model has the form:

$$\begin{aligned}
 H = & \epsilon_B \sum_{i\sigma} \eta_i f_{i\sigma}^\dagger f_{i\sigma} + \epsilon_{B'} \sum_{i\sigma} (1 - \eta_i) m_{i\sigma}^\dagger m_{i\sigma} \\
 & + H_{kin}\{\eta\} + J \sum_{i\alpha\beta} \eta_i \mathbf{S}_i \cdot f_{i\alpha}^\dagger \vec{\sigma}_{\alpha\beta} f_{i\beta} - \mu \hat{N} \\
 & + J_{AF} \sum_{\langle i,j \rangle} \eta_i \eta_j \mathbf{S}_i \cdot \mathbf{S}_j
 \end{aligned} \tag{1}$$

f is the electron operator on the magnetic B site and m is the operator on the non-magnetic B’ site. ϵ_B and $\epsilon_{B'}$ are onsite energies, at the B and B’ sites respectively. $\epsilon_B - \epsilon_{B'}$ is a ‘charge transfer’ energy. H_{kin} is the electron hopping term: $-t_1 \sum_{\langle i,j \rangle \sigma} \eta_i \eta_j f_{i\sigma}^\dagger f_{j\sigma} - t_2 \sum_{\langle i,j \rangle \sigma} (1 - \eta_i)(1 - \eta_j) m_{i\sigma}^\dagger m_{j\sigma} - t_3 \sum_{\langle i,j \rangle \sigma} (\eta_i + \eta_j - 2\eta_i \eta_j)(f_{i\sigma}^\dagger m_{j\sigma} + h.c)$. The t ’s are all nearest neighbour hopping amplitudes, and for simplicity we set $t_1 = t_2 = t_3 = t$ here. \mathbf{S}_i is the core spin on the site \mathbf{R}_i , with $|\mathbf{S}_i| = 1$. J is the Hund’s coupling on the B sites, and we use $J/t \gg 1$. When the up-spin core levels are fully filled, *e.g.*, Fe $t_{2g\uparrow}$ and $e_{g\uparrow}$ in SFMO, the conduction electron is forced to be *antiparallel* to the core spin. We have used $J > 0$ to model this situation. For the present study we have set¹⁹ the *effective* level difference $\epsilon_B - J/2 - \epsilon_{B'} = 0$. The chemical potential μ is used to control the electron density, and \hat{N} is the total electron density operator. We study one point in the A type window, and another in the G type window. We also explore the transition from FM to A type order.

When two magnetic atoms can be on neighbouring sites, we also have to consider the *antiferromagnetic* coupling J_{AF} between nearest neighbour B sites.

It has been well established now that the antisite disorder does not involve ‘random’ exchange of B and B’ ions, but follows a correlated pattern^{12,13}. A periodic B-B’ pattern is interrupted by a line-like defect, where BB or B’B’ adjoin each other, and beyond this boundary one obtains another domain but with a phase slippage with respect to the first one. The line defect is an antiphase boundary. If a fraction x of atoms are ‘mislocated’ with respect to the ideal ordered structure, these atoms themselves are organised into domains, and do not act as simple ‘point defects’.

We generate the correlated patterns by studying a lattice gas model²⁰, with poor annealing to prevent long

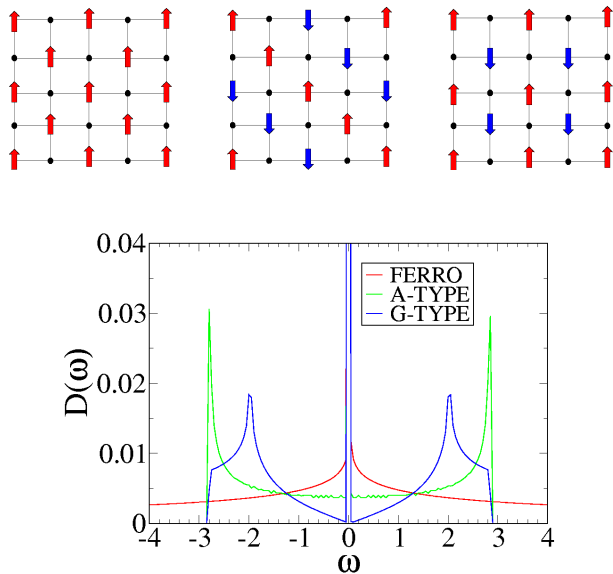


FIG. 1: Top: The three magnetic phases in the structurally ordered 2D double perovskite model. Left: ferromagnetic (FM), center: A type antiferromagnet, right: G type antiferromagnet. These occur with increasing electron density. The moments are on the B sites. We have not shown the induced moments on the B' sites. Bottom: Electronic density of states for the ferromagnetic, A and G type ordered phases in the structurally ordered background.

range order. Briefly, the $\{\eta_i\}$ configuration arise from:

$$H_{eff}\{\eta\} = -V \sum_{\langle ij \rangle} \eta_i (1 - \eta_j) \quad (2)$$

The η are coupled only between nearest neighbour sites. The ground state in this model corresponds to $\eta = 1, 0, 1, 0, \dots$ along each axis, *i.e.*, B, B', B, B'.. $V > 0$ is a measure of the ordering tendency, and sets the temperature for long range B-B' order if the system were allowed to equilibrate.

We used different ‘annealing time’, τ_{ann} , and annealing temperature, T_{ann} , to generate the ASD configurations. The ASD structures are characterised in terms of the following indicators: (i) The structural ‘order parameter’ $S = 1 - 2x$, where x is the fraction of B (or B') atoms that are on the wrong sublattice. (ii) The degree of short range order, characterised by the probability, p , of having nearest neighbour pairs that are B-B'. (iii) The correlation length ξ in these structures, computed from the width of the ordering peak.

For a given $\{\eta_i\}$ configuration, generated at some T_{ann} and τ_{ann} , we solve for the magnetic properties, and electronic properties averaged over equilibrium magnetic configurations, via a cluster based Monte Carlo technique²³. Electronic properties are calculated after equilibration by diagonalizing the full system.

The electronic conductivity is calculated using the Kubo formula, computing the matrix elements of the current operator. The ‘dc conductivity’ is the low frequency

average, $(1/\Delta\omega) \int_0^{\Delta\omega} \sigma(\omega) d\omega$ of the optical conductivity. This is averaged over thermal configurations and disorder, as appropriate. We use $\Delta\omega = 0.05t$.

IV. RESULTS

A. The clean limit

In the absence of antisite disorder there are no AF superexchange interactions in the system, and the magnetic order is decided by minimisation of the electronic energy. We reproduce the model for the ordered DP, below, for ease of reference:

$$H_{ord} = \epsilon_B \sum_{i \in B, \sigma} f_{i\sigma}^\dagger f_{i\sigma} + \epsilon_{B'} \sum_{i \in B', \sigma} m_{i\sigma}^\dagger m_{i\sigma} - \mu \hat{N} \\ - t \sum_{\langle ij \rangle < \sigma} f_{i\sigma}^\dagger m_{j\sigma} + J \sum_{i \in A, \alpha\beta} \mathbf{S}_i \cdot f_{i\alpha}^\dagger \vec{\sigma}_{\alpha\beta} f_{i\beta}$$

For $J/t \gg 1$ this model supports three collinear phases (in 2D). The FM state gives way to A type (line like) order with increasing electron density, and finally to a G type state. These have been discussed earlier⁸, we reproduce the magnetic configurations, top row in Fig.1, and the electronic density of states below. We have set $(\epsilon_B - J/2) - \epsilon_{B'} = 0$.

The FM state is preferred at low n , since it has the largest bandwidth. The A type state has lower bandwidth, but with large density of states near the band edge. The FM becomes unstable at $n \sim 0.45$. The A type state is stable for $n \geq 0.58$, and between these we have a phase separation (PS) window. Similarly the A to G transition involves a PS window. The PS windows narrow with increasing T and vanish as $T \rightarrow T_c$. The thermal transitions and the PS windows are shown in Fig.2.

Broadly, the task would be to extend this phase diagram to finite antisite disorder. Instead of attempting

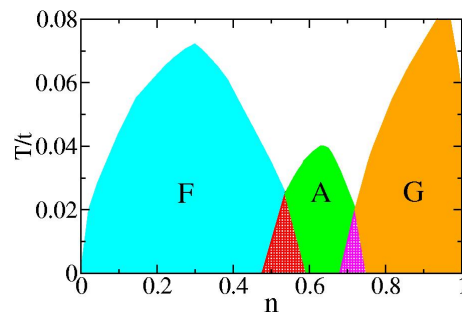


FIG. 2: Colour online: Phase diagram for the non disordered double perovskite. We only show the region $n = [0, 1]$. From $n = 1$ to $n = 2$ one populates the non-dispersive B' level, and the magnetic state is G type. The $n = [2, 3]$ window is a symmetric version of the $n = [1, 2]$ region. The regions between the phases indicate phase separation. The results are obtained via MC on a 40×40 lattice.

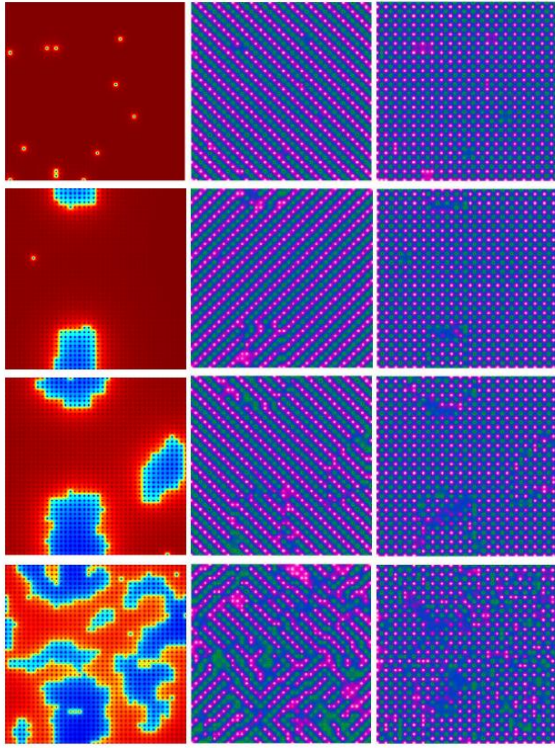


FIG. 3: Colour online: Antiphase domains and corresponding antiferromagnetic phases. The left column shows the domain pattern in the ASD background, with structural order parameter $S = 0.98, 0.76, 0.50, 0.08$ as we move from top to bottom. The middle column shows the A type AF phase on this structural motif, while the right column shows the G type phase. The magnetic correlations are characterised via the overlap factor $g_i = \mathbf{S}_0 \cdot \mathbf{S}_i$, where \mathbf{S}_0 is the left lower corner spin in the lattice.

to map out the disorder dependence at *all densities* we choose two representative densities, $n \sim 0.65$ in the A type window, and $n \sim 0.95$ in the G type region, to clarify the impact of disorder. We also explore the effect of ASD on the phase separation window since it would be encountered in any attempt to electron dope the ferromagnet.

B. Disorder configurations

We study four families, with progressively increasing antisite disorder. Each family arises from annealing the lattice gas model for some time τ_{ann} at temperature T_{ann} . A representative configuration from each family is shown in the first column in Fig.3. They have a fraction of mislocated sites: $x = 0.01, 0.12, 0.25, 0.46$. The fraction of course varies somewhat from sample to sample within each family. Our ‘disorder average’ for magnetic and electronic properties is performed typically over 10 configurations within each family.

The structural ‘order parameter’ $S = 1 - 2x$ is

0.98, 0.76, 0.50, 0.08 for these four families. Since the configurations emerge from an annealing process, the spatial correlations in the structure are much stronger than the S value would suggest. In the absence of information about spatial correlations, the probability p of having a BB’ nearest neighbour bond is $p = x^2 + (1 - x)^2 = (1/2)(1 + S^2)$. The two terms, x^2 and $(1 - x)^2$, arise from having both atoms on the ‘wrong’ sublattice or ‘right’ sublattice respectively. For the S values in our configurations these numbers are $\sim 0.98, 0.79, 0.63, 0.50$. In our case the structures are spatially correlated, so the probability of BB’ nearest neighbours is much higher than the estimates, above, from an ‘uncorrelated distribution’. By analysing our configurations we obtain: $p \sim 0.98, 0.97, 0.95, 0.86$, indicating a high degree of short range order. We also estimated the ‘correlation length’ ξ associated with the domain structures, from a Lorentzian fit to the B-B’ structure factor of the form $S_{BB'}(\mathbf{q}) \sim \xi^{-1} / ((q_x - \pi)^2 + (q_y - \pi)^2 + \xi^{-2})$. This yields $\xi \sim 6.6, 5.9, 4.8, 3.6$.

Overall, the disorder in these systems should be characterised in terms of two variables: S , which is a gross measure of order, and p (or ξ) which quantify short range correlation. In general, physical properties would depend on both of these and not simply S .

C. Magnetic order with antisite disorder

In the FM case it is simple to see that the presence of AF superexchange at the APB would tend to align spins in opposite directions across an antiphase boundary. The system breaks up into up and down spin domains. Suppose the ‘up spin’ domains correspond to the correctly located sites and are the ‘majority’. The net magnetisation is proportional to the volume difference between the correctly located and ‘mislocated’ regions. If the degree of mislocation is x , then the normalised magnetisation $M = (1 - x) - x = 1 - 2x = S$. In the magnetic structure factor $D(\mathbf{q})$, the FM peak is at $\mathbf{Q}_F = \{0, 0\}$. By definition $D(\mathbf{Q}_F) = M^2$, and from the domain argument this is simply S^2 . This dependence is well established experimentally²¹, and also observed by us²².

For the A type phase, studied on the same antisite structures as the FM, the nature of local magnetic order is more subtle. For the clean A-AF the order is at *two possible pairs* of wavevectors, $\mathbf{Q}_{A1} = \{\pi/2, \pi/2\}$ and $\mathbf{Q}_{A2} = \{3\pi/2, 3\pi/2\}$, or $\mathbf{Q}_{A3} = \{\pi/2, 3\pi/2\}$ and $\mathbf{Q}_{A4} = \{3\pi/2, \pi/2\}$. We have set the lattice spacing $a_0 = 1$ on the DP lattice. The two sets arise due to the two possible diagonals along which the FM stripes can order. Within each set there are two \mathbf{Q} values because half the sites in the DP lattice are non-magnetic, and the spin field has to have nodes there. In the clean system either $\{\mathbf{Q}_{A1}, \mathbf{Q}_{A2}\}$ or $\{\mathbf{Q}_{A3}, \mathbf{Q}_{A4}\}$ are picked. In a disordered system all four can show up, as in the middle column bottom row in Fig.3. For the G type phase the order is at the single pair: $\mathbf{Q}_{G1} = \{\pi, 0\}$ and $\mathbf{Q}_{G2} = \{0, \pi\}$.

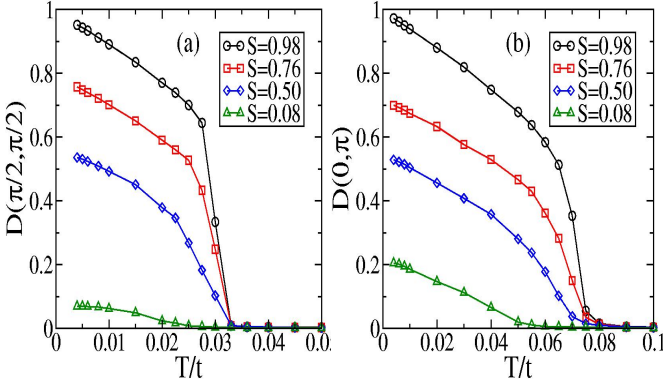


FIG. 4: Colour online: Magnetic order in the A type and G type phases with ASD. The results are based on MC on 40×40 systems, and averaged typically over 10 configurations for each value of S .

The middle and right columns in Fig.3 show A type and G type order, respectively, for progressively increasing ASD. Fig.4 quantifies the suppression of the ordering peak in $D(\mathbf{q})$, after disorder averaging over copies with roughly fixed degree of mislocation.

We will analyse the structure factor, $D(\mathbf{q})$, in terms of the domain pattern. $D(\mathbf{q})$ is related to the Fourier transform of the spin configuration:

$$D(\mathbf{q}) = \frac{1}{V^2} |\vec{f}(\mathbf{q})|^2$$

$$\vec{f}(\mathbf{q}) = \sum_{\mathbf{R}_i} \mathbf{S}_i e^{i\mathbf{q} \cdot \mathbf{R}_i}$$

where V is the total volume of the system.

For collinear order, where the spin projection is only on the z axis, the spin vector can be replaced by S_i . If we imagine the spin configuration to be broken up into domains, indexed by a label α , say, then, for collinear phases, $\vec{f}(\mathbf{q}) = \hat{z} f(\mathbf{q})$ and:

$$f(\mathbf{q}) = \sum_{\alpha} \sum_{\mathbf{R}_i^{\alpha}} S_i e^{i\mathbf{q} \cdot \mathbf{R}_i^{\alpha}} = \sum_{\alpha} f_{\alpha}(\mathbf{q}) \quad (3)$$

where the sum runs over the domains, and the \mathbf{r}_i^{α} are coordinates within a domain. This shows that $f(\mathbf{q})$ gets additive contributions from various domains, with phase factors that we will soon clarify. The formulation above holds as long as (a) there is no significant non collinearity and (b) $\xi \gg 1$, *i.e.*, we can ignore ‘interfacial’ spins which may be hard to assign to any particular domain.

1. A type order

For weak to moderate ASD we observe that the system prefers FM stripes along any single diagonal, albeit with phase slippage between the stripes to accommodate the effect of J_{AF} . This is true for $S = 0.98, 0.76$ and 0.50 , the top three rows in the middle column in Fig.3.

Domains which are translated with respect to the reference domain have relative displacement $\delta \mathbf{r}_{\alpha} = \hat{x} a_0$ or $\hat{y} a_0$. The order *within* all domains is similar. So, the contribution of each domain at the ordering wavevector, \mathbf{Q} , will be proportional to the domain volume, and involve a phase factor:

$$f_{\alpha}(\mathbf{Q}) = V_{\alpha} e^{i\mathbf{Q} \cdot \delta \mathbf{r}_{\alpha}} f_0(\mathbf{Q})$$

where $f_0(\mathbf{Q})$ is the normalised reflection in the perfectly ordered system. For the $\mathbf{Q} = \mathbf{Q}_{A1} = \{\pi/2, \pi/2\}$ peak, the phase factor is $e^{i\pi/2}$ irrespective of whether the domain is x displaced or y displaced. So, all the ‘mislocated’ sites, grouped into domains, contribute $V_{mis} e^{i\pi/2} f_0(\mathbf{Q})$, where V_{mis} is the total volume of mislocated regions.

Adding the contribution from the majority domains, which are undisplaced, we obtain:

$$f(\mathbf{Q}_{A1}) = ((V - V_{mis}) + V_{mis} e^{i\pi/2}) f_0(\mathbf{Q}_{A1})$$

Remembering that $V_{mis}/V = x$, the volume normalised structure factor peak is

$$D(\mathbf{Q}_{A1}) = |(1 - x) + e^{i\pi/2} x|^2 = \frac{1}{2}(1 + S^2)$$

This is roughly consistent with the S dependence of the $T \rightarrow 0$ structure factor in Fig.4.(a). It is *distinctly slower* than the suppression of order in the ferromagnet, where $D(\mathbf{Q}_F) \sim S^2$.

At larger ASD however, the system has short stripes oriented along *both* diagonals, see bottom row middle panel in Fig.3. These domains have magnetic peaks at $\mathbf{Q}_{A3}, \mathbf{Q}_{A4}$ and not at $\mathbf{Q}_{A1}, \mathbf{Q}_{A2}$. Even assuming that the ‘majority’ domains all contribute $(1 - x)f_0(\mathbf{Q}_{A1})$, we notice that the mislocated regions require classification into two groups: those contributing at $\mathbf{Q}_{A1}, \mathbf{Q}_{A2}$ with volume fraction y , say, and those at $\mathbf{Q}_{A3}, \mathbf{Q}_{A4}$ with volume fraction $x - y$. In that case the peak at \mathbf{Q}_{A1} would be

$$D(\mathbf{Q}_{A1}) = |(1 - x) + e^{i\pi/2} y|^2$$

The $(x - y)$ fraction makes no contribution to the peak, and that weight is ‘lost’. Notice that $x \geq y \geq 0$, and it is not possible to write $D(\mathbf{Q}_{A1})$ purely in terms of S . We could write the expressions for the structure factor at the other three \mathbf{Q} as well, and they will all depend on both x and y . This is a general feature of magnetic states where the order can locally pick out different orientations.

We can make some headway in the strong disorder limit, $x = 1/2, S = 0$, by assuming that there are four kinds of domains, with roughly equal area. There would be two families of $\{\mathbf{Q}_{A1}, \mathbf{Q}_{A2}\}$ domains, each with $1/4$ the system volume, and a relative phase shift $\pi/2$. Similarly there would be two families of $\{\mathbf{Q}_{A3}, \mathbf{Q}_{A4}\}$ domains, each with volume $1/4$, and relative phase shift $\pi/2$. In this case the \mathbf{Q}_{A1} peak, for example, in $D(\mathbf{Q})$ will be:

$$D(\mathbf{Q}_{A1}) = |1/4 + e^{i\pi/2}/4|^2 = 1/8$$

This is not very far from $D(\mathbf{Q}_{A1}) \sim 0.1$ that we obtain from the Monte Carlo. Other peaks, at $\mathbf{Q}_{A2}, \mathbf{Q}_{A3}$, *etc.*, would have similar magnitude.

2. G type order

G type order occurs at the combination $\{\mathbf{Q}_{G1}, \mathbf{Q}_{G2}\} : \{\{0, \pi\}, \{\pi, 0\}\}$. As before the relative displacement of the domains can be only $\hat{x}a_0$ or $\hat{y}a_0$. Suppose we are computing the structure factor at \mathbf{Q}_{G1} then all domains will contribute, but with following phase factors: zero if the domain is not mislocated ($\delta\mathbf{r} = 0$), zero again if the domain is \hat{x} displaced, and $e^{i\pi} = -1$ if the domain is \hat{y} displaced.

In *two domain* systems, as in the second row in Fig.3, the mislocated domain is either x displaced or y displaced. For copies with x displacement the contribution at \mathbf{Q}_{G1} will be $|(1-x) + x|^2 = 1$, while for y displacement it will be $|(1-x) + e^{i\pi}x|^2 = (1-2x)^2 = S^2$. Averaging the *structure factor* over copies would lead to $D(\mathbf{Q}_{G1}) = (1/2)(1 + S^2)$. This is roughly what we observe in our Fig.4.(b) at $T = 0$.

In large systems, where there will be many domains, we can assume that half the mislocated domains are x displaced and half y displaced. In that case the structure factor would be

$$D(\mathbf{Q}_{G1}) = |(1-x) + x/2 + e^{i\pi}x/2|^2$$

Using $1 - 2x = S$ this leads to

$$D(\mathbf{Q}_{G1}) = (1/4)(1 + S)^2$$

For $S \rightarrow 0$ this gives 0.25, not far from ~ 0.20 that we obtain from our configurations.

This reveals that for both A and G type order even when *half the sites are mislocated*, *i.e.*, one has maximal antisite disorder, there is a surviving peak in the structure factor. All these of course assumed that the structural pattern had a high degree of spatial correlation so that one can meaningfully talk of domains. We should have $1 - p \ll 1$, or structural correlation length $\xi \gg a_0$. If the structures were fragmented to a random alloy then the results above would not hold. We have checked this explicitly.

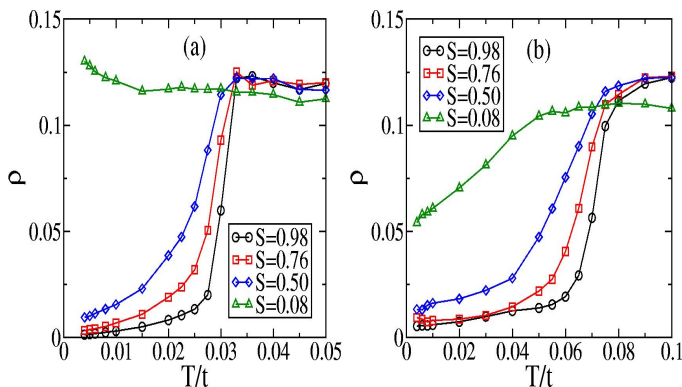


FIG. 5: Colour online: Resistivity in the A type and G type phases with ASD. The results for each S are averaged over 10 realisations of disorder.

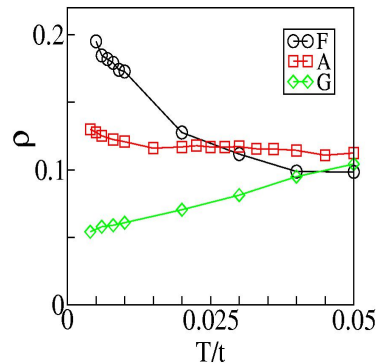


FIG. 6: Colour online: Comparison of the resistivity in the FM, A and G type correlated phases in samples with the lowest degree of order $S = 0.08$.

D. Transport with antisite disorder

All the three phases, FM, A type, and G type, in the 2D double perovskite model are metallic in the clean limit. The electronic states are extended, and there is a finite density of states at the Fermi level. In the absence of antisite disorder the resistivity, $\rho(T)$, in all three have similar temperature dependence. The resistivity increases rapidly as T increases towards T_c , Fig.5 and our earlier work²² on the FM, and ‘saturates’ at high temperature. A Fisher-Langer type²⁴ phenomenology can qualitatively describe the transport.

Weak disorder leads to an increase in the residual resistivity of the A and G type phases, see Fig.5, as observed earlier for the FM. The sharp resistive transition observed in the clean limit ($S = 0.98$) is also gradually broadened with increasing disorder. There is however a key difference with respect to the FM phase when we move to strong disorder.

In the 2D case our results²² on the FM suggest an insulating $T = 0$ state beyond a critical disorder, with $d\rho/dT < 0$. At the highest disorder, $S = 0.08$, $\rho(T)$ in the A type AF remains essentially flat down to $T = 0$, while in the G type phase there is still a low temperature *downturn*. While these are finite size results, we argue below why there is an intrinsic reason for transport in the AF phases to be less sensitive to antisite disorder and domain formation. This is related to the nature of electronic wavefunctions in these phases. We consider the two phases in succession below.

In the A type phase the core spin order involves diagonal stripes. ‘Up-spin’ electrons delocalise on down-spin stripes which involve one B diagonal and the two adjacent B’ lines. ‘Down-spin’ electrons delocalise on up-spin stripes. The down and up stripes share a common B’ line. The essential feature is that the electronic wavefunctions are quasi-one dimensional. The introduction of antisite disorder leads to two effects: (i) it hinders propagation along the stripe, and (ii) allows scattering between the stripes leading to an ‘expansion’ of the wavefunction in the transverse direction. On its own, the first effect

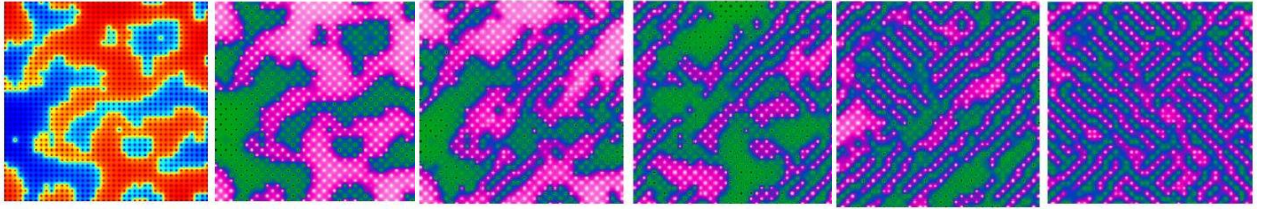


FIG. 7: Colour online: Magnetic correlations with increasing electron density as one traverses the coexistence regime in an antisite disordered background. The first panel shows the structural pattern arising from the ASD. Panel 2 shows the spin correlations at $\mu = \mu_{FM} = -1.8$, where the ground state is a (domain) ferromagnet. The extreme right is for $\mu = \mu_{AF} = -1.4$, where the system has only A type AF correlations. As μ increases from μ_{FM} to μ_{AF} the pattern exhibits coexistence of short range FM and AF correlations.

would have suppressed conduction, but the new matrix element between stripes allows a transverse pathway for delocalisation. In contrast to the FM case there is no ‘confinement’ of the wavefunctions to specific domains, and the two competing effects above lead to a finite resistivity (at least a much weaker upturn) even at strong disorder.

In the clean G type phase the system can be viewed as two interpenetrating square lattices, one with up spin B sites, the other with down spin B sites. The electrons delocalise via the B’ sites, and each B’ site hosts both up and down electron states. Electrons in both spin channels are delocalised over the whole system in the absence of ASD. The presence of antisite domains leads to scattering but no confinement of electrons to the domains. Due to the inherently 2D character of the G type electronic states, in contrast to quasi-1D for A type, the system has a lower resistivity.

We contrast the resistivity of the three phases in Fig.6 for the case of maximum disorder that we have studied. These are configurations with $S \sim 0.08$, but, as we have noted, with a fairly high degree of local correlation. The FM has a clear low T upturn due to the confinement of electrons into domains or pathways created by the ASD. The A and G type electronic states, in either spin chan-

nel, are *not confined* to the magnetic/structural domains, and the resistivity remains comparatively lower. The high temperature resistivity is determined by spin disorder scattering, depends weakly on carrier density (the FM, A and G phases have different n), and is almost temperature independent.

E. Phase coexistence

In the clean limit, the increase of electron density by doping the FM would encounter a window of phase separation. A homogeneous state is not allowed for $0.45 \leq n \leq 0.58$ and this (idealised) system would break up into macroscopic regions having densities $n \sim 0.45$ and $n \sim 0.58$. This pathology is avoided by long range Coulomb interactions or quenched disorder. For the antisite disordered configurations that we are considering the ASD itself controls the pattern of spatial coexistence.

Fig.7 shows the magnetic correlations in a fixed antisite background for changing electron density. The leftmost panel is the structural pattern, showing the antisite domains. The next five snapshots correspond to increasing chemical potential, μ , and consequently the electron density. The first panel in this set is a (domain) ferromagnet at $n < 0.45$, the second shows emergence of stripes along with the FM regions. The FM regions shrink and the linelike patterns become more prominent in the third panel. The fourth and fifth panel complete the evolution, with FM correlations completely replaced by stripes (of both orientation) as in the bottom of middle column in Fig.3. The evolution of the particle density with μ , and the rapid change near the phase separation window, are shown in Fig.8.

V. CONCLUSIONS

We have studied the survival of the antiferromagnetic double perovskite phases in the presence of spatially correlated antisite disorder. We observe that antisite disorder affects the antiferromagnetic order much less strongly than it affects ferromagnetism. For a given structural order parameter S , the A type AF structure factor follows

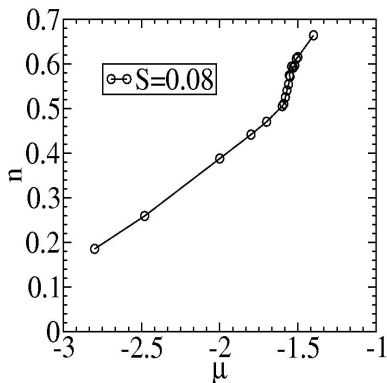


FIG. 8: Colour online: The variation of electron density with chemical potential as the FM to A type AF crossover is traversed in a high ASD sample ($S = 0.08$).

$D_A \sim (1 + S^2)/2$, in contrast to $D_F \sim S^2$ in the ferromagnet, while the G type phase follows $D_G \sim (1 + S)^2/4$. So, despite the possibility of large antisite disorder at the high electron doping needed to observe the AF phases, there is certainly hope of observing these magnetic structures. The AF states are metallic, and the electronic wavefunctions in these phases continue to be spatially extended even at large disorder. Antisite disorder increases the residual resistivity, but, unlike the ferromagnet, we did not observe any insulating regime. The field response

of these AF metals is also fascinating, and will be separately discussed.

Acknowledgements: We thank T. Saha Dasgupta, P. Sanyal and S. Ray for early discussions and Rajarshi Tiwari for collaboration on related issues. We acknowledge use of the Beowulf Cluster at HRI. PM acknowledges support from a DAE-SRC Outstanding Research Investigator Award, and the DST India through the Indo-EU ATHENA project.

-
- ¹ K.-I. Kobayashi, T. Kimura, H. Sawada, K. Terakura and Y. Tokura, *Nature* **395**, 677 (1998).
 - ² D. D. Sarma, *Current Op. Solid St. Mat. Sci.*, **5**, 261 (2001).
 - ³ D. Serrate, J. M. de Teresa and M. R. Ibarra, *J. Phys. Cond. Matt.* **19**, 023201 (2007).
 - ⁴ D. D. Sarma, P. Mahadevan, T. Saha-Dasgupta, S. Ray, and A. Kumar, *Phys. Rev. Lett.* **85**, 2549 (2000).
 - ⁵ A. Chattopadhyay and A. J. Millis, *Phys. Rev. B* **64**, 024424 (2001).
 - ⁶ E. Dagotto, *Science*, **309**, 257 (2005).
 - ⁷ Y. Tokura, *Rep. Prog. Phys.* **69**, 797 (2006).
 - ⁸ P. Sanyal and P. Majumdar, *Phys. Rev. B* **80**, 054411 (2009).
 - ⁹ P. Sanyal, H. Das and T. Saha-Dasgupta, *Phys. Rev. B* **80**, 224412 (2009).
 - ¹⁰ T. K. Mandal, C. Felser, M. Greenblatt, and J. Kuble, *Phys. Rev. B* **78**, 134431 (2008).
 - ¹¹ R. Tiwari and P. Majumdar, unpublished.
 - ¹² T. Asaka, X. Z. Yu, Y. Tomioka, Y. Kaneko, T. Nagai, K. Kimoto, K. Ishizuka, Y. Tokura, and Y. Matsui, *Phys Rev B* **75**, 184440 (2007).
 - ¹³ C. Meneghini, Sugata Ray, F. Liscio, F. Bardelli, S. Mobilio, and D. D. Sarma, *Phys. Rev. Lett.* **103**, 046403 (2009).
 - ¹⁴ Y. H. Huang, M. Karppinen, H. Yamauchi, and J. B. Goodenough, *Phys. Rev. B* **73**, 104408 (2006), Y. H. Huang, H. Yamauchi, and M. Karppinen, *Phys. Rev. B* **74**, 174418 (2006).
 - ¹⁵ Navarro, L. Balcells, F. Sandiumenge, M. Bibes, A. Roig, B. Martnez and J. Fontcuberta, *J. Phys. Cond. Matt* **13**, 8481 (2001), J. Navarro, J. Nogues, J. S. Munoz, and J. Fontcuberta, *Phys. Rev. B* **67**, 174416 (2003).
 - ¹⁶ J. L. Alonso, L. A. Fernandez, F. Guinea, F. Lesmes, and V. Martin-Mayor, *Phys. Rev. B* **67**, 214423 (2003).
 - ¹⁷ D. Sanchez, J. A. Alonso, M. Garcia-Hernandez, M. J. Martinez-Lopez, M. T. Casais and J. L. Martinez, *J. Mater. Chem.* **13**, 1771 (2003).
 - ¹⁸ S. Ray *et al.*, unpublished.
 - ¹⁹ This refers to a situation where the effective level difference between B and B' is zero. If this difference were comparable to t one would begin to see additional 'potential scattering' effects arising from the antiphase boundaries, enhancing the overall resistivity. The present study focuses purely on how magnetic order affects transport.
 - ²⁰ P. Sanyal, S. Tarat and P. Majumdar, *Eur. Phys. J. B* **65**, 39 (2008).
 - ²¹ C. Frontera and J. Fontcuberta, *Phys. Rev. B* **69**, 014406 (2004).
 - ²² V. Singh and P. Majumdar, arXiv 0105653.
 - ²³ S. Kumar and P. Majumdar, *Eur. Phys. J. B* **50**, 571 (2006)
 - ²⁴ M. E. Fisher and J. S. Langer, *Phys. Rev. Lett.* **20**, 665 (1968).